RECENT TECHNOLOGIES FOR THE RELIABILITY AND PERFORMANCE OF MECHANICAL-DRIVE STEAM TURBINES IN ETHYLENE PLANTS

by

Tomoyoshi Sasaki

Manager, Turbine Design Section

Satoshi Hata

Manager, Turbine Design Section

Masahiro Kobayashi

Senior Engineer, Turbine Design Section

and

Osamu Isumi

Engineer, Turbine Design Section

Mitsubishi Heavy Industries, Ltd.

Hiroshima, Japan

Tomoyoshi Sasaki is a Manager of the Turbine Design Section in the Power Systems & Turbomachinery Engineering Department, Mitsubishi Heavy Industries, Ltd., in Hiroshima, Japan. He has been with them for the past 26 years. He has been in the R&D and detail designing of mechanical drive and generator drive steam turbines for 17 years.

Mr. Sasaki has B.S. and M.S. degrees (Mechanical Engineering) from Kyushu University.

Satoshi Hata is a Manager of the Turbine Design Section in the Power Systems & Turbomachinery Engineering Department, Mitsubishi Heavy Industries, Ltd., in Hiroshima, Japan. He has had experience with R&D for nuclear uranium centrifuges, turbomolecular pumps, and heavy duty gas turbines and steam turbines for 17 years.

Mr. Hata has B.S. and M.S. degrees (Mechanical Engineering) from Kyushu Institute of Technology.

Masahiro Kobayashi is the Senior Engineer of the Turbine Design Section in the Power Systems & Turbomachinery Engineering Department, Mitsubishi Heavy Industries, Ltd., in Hiroshima, Japan. He has had experience with R&D for gas turbines and steam turbines for 14 years.

Mr. Kobayashi has B.S. and M.S. degrees (Mechanical Engineering) from Yamaguchi University.

ABSTRACT

Recently, large capacity ethylene plants have been constructed in the world and the trend for the capacity of these plants is increasing. At present it reaches up to about one million tons per year and more. Accordingly, the mechanical drive steam turbines in the ethylene plants become larger and their shaft end power increases.

Also the requirement for long-term continuous operation and high performance of these turbines becomes more important year by year in order to save operation and maintenance costs.

This paper focuses on mechanical drive steam turbines in ethylene plants and introduces the recent technologies for reliability and performance improvement. Some of these technologies have already been successfully applied to actual steam turbines.

INTRODUCTION

As the plant capacity increases, large size governing valves have to be designed for steam turbines since the fluid exciting force around the governing valve will increase in proportion to the steam flow. Unexpected large fluid exciting force sometimes causes abrasion between the valve and the stem. Both calculations and model tests were carried out in order to investigate the stabilization of chattering phenomena and to evaluate damping coefficient, fluid exciting force, and the risk of abrasion based on design criteria.

It was confirmed, from the result of an overhaul after eight years of continuous operation at an ethylene plant, that Cr-TiN ion coating was a useful solution in preventing profile damage by erosion in low-pressure stage blades. Furthermore, a stellite welding technique by the plasma transfer arc (PTA) method has been developed as an alternative method suitable for severe drainage erosion. By laboratory examination of this method, the welding condition, erosion characteristic, and endurance limit were confirmed.

In order to improve the high-pressure stage efficiency further, the application of a bow nozzle (three-dimensional nozzle) was studied. Due to the cost and the reliability advantages with adoption of the cast bow nozzle, the area adjustment method was applied by the wide orientation of the nozzle outlet angle without a profile change. The performance of this advanced bow nozzle was confirmed by three-dimensional fluid analysis and model test.

The improved sealing effect of the slanting seal was confirmed by an air cascade test for flow visualization of the slanting seal and for measuring leakage flow.

RELIABILITY OF CAPACITY INCREASE

During this decade, the capacity of ethylene plants has tended to increase constantly as shown in Figure 1. The capacity of the high-pressure stage of the steam turbine is especially increasing in comparison with that of the low-pressure stage. To meet the capacity increase in the near future, it is necessary to develop large inlet flow steam turbines for ethylene plants, keeping in mind that long-term

continuous operation is also required to save maintenance cost and to minimize production loss due to periodic shut downs.

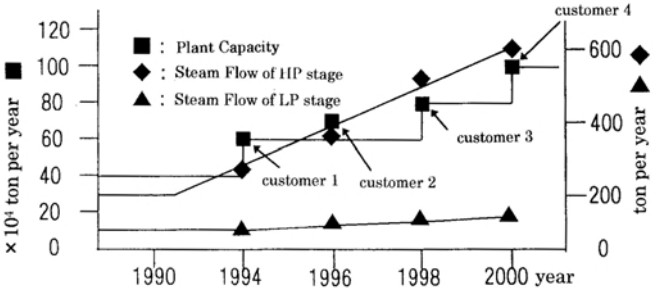

Figure 1. Capacity Tendency of Ethylene Plant.

To achieve both large flow capacity and long term reliability, the abrasion between the valve stem and the bushing and the chattering phenomenon of the governing valve were considered and design criteria were developed. The design specifications and the cross section of the governing valve portion are shown in Figure 2 comparing both the developed and conventional turbines.

	Developed type	Conventional type
Valve	Semi-independent type	Independent type
Dia. × number	Φ 90 × 4 valves	Φ 90 × 4 valves
valve chest	Solid casing type	Separate casing type
U-tube	not apply	apply
Inlet steam flow	620T/H	545T/H
Inlet steam press.	130kg/cm²	123kg/cm²
Inlet steam temp.	530℃	510℃

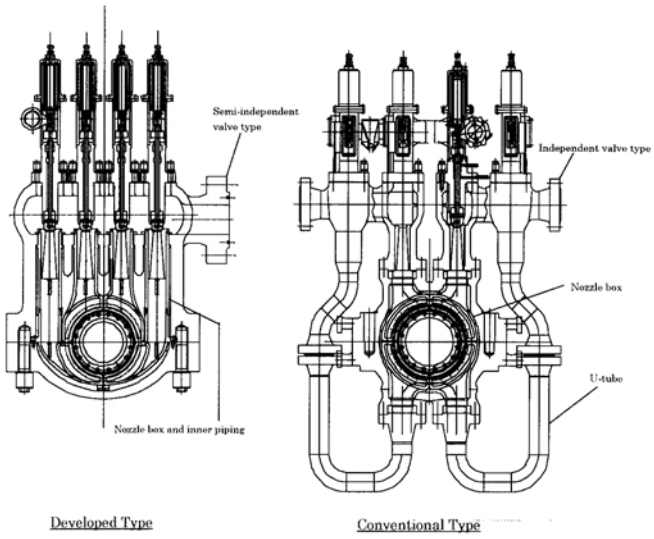

Figure 2. Sectional Drawing of Governing Valve for Developed and Conventional Turbine.

Abrasion Between the Valve Stem and the Bushing

The fluid force on the valve is described as the following equation:

$$F_{D,L} = \frac{1}{2} C_{D,L} \cdot \rho \cdot A \cdot u^2 \tag{1}$$

where:
$F_{D,L}$ = Fluid force on governing valve
$C_{D,L}$ = Drag coefficient
ρ = Density of fluid
A = Force subjected area
u = Velocity

The fluctuating force on the valve is found by differential calculus of the Equation (1):

$$\begin{aligned} \Delta F_{D,L} &= C_{D,L} \cdot \rho \cdot A \cdot u \cdot \Delta u \\ &= C_{D,L} \cdot \mu \cdot A \cdot \frac{Re}{D} \cdot \Delta u \end{aligned} \tag{2}$$

where:
$\Delta F_{D,L}$ = Fluctuating fluid exciting force on governing valve
Δu = Fluctuating velocity
Re = Reynolds number
D = Valve diameter

Based on Equation (2), the fluid exciting force on the governing valve by steam flow is estimated by the Equation (3):

$$\Delta F_{D,L} = \mu \cdot \frac{A}{D} \cdot f(\phi) \cdot Re^m \cdot Ma^n \tag{3}$$

where:
μ = Viscosity coefficient
ϕ=L/D = Nondimensional valve lift
L = Valve lift
$f(\phi)$ = Function of nondimensional valve lift, ϕ
Ma = Mach number
m, n = Constant multiplier number

In order to determine the values of $f(\phi)$, m, and n, an air model test was carried out by the test setup shown in Figure 3. The test valve is shown in detail in Figure 4, in which the three-direction load-cell was installed and the fluid exciting force was measured for the right angle direction of the valve axis. In this test, the pressure ratio between the inlet and outlet valve and the opening ratio of the valve were chosen as the test parameters. The typical measured and fast Fourier transform (FFT) analyzed fluid exciting force spectrum for each valve lift is shown in Figure 5.

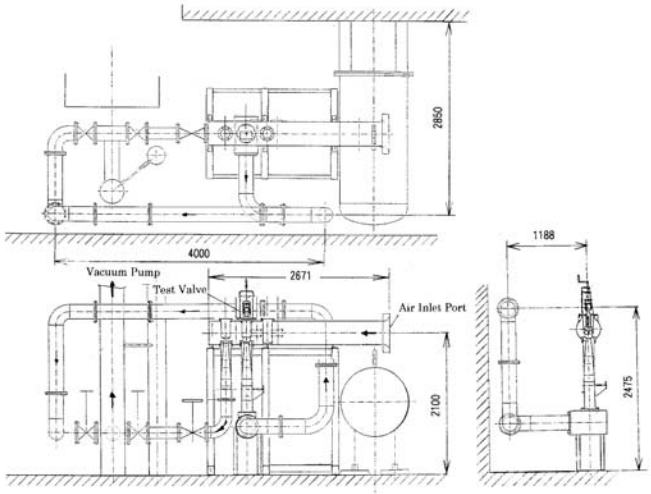

Figure 3. Test Device.

The relation of Mach number $(Ma)^n$, the ratio of $(Re)^m$, and $\Delta F_{D,L}$ are plotted in Figure 6. m and n can be found by using Equation (3) based on these measured data. Also, in the same manner, the maximum value of $f(\phi)$ can be obtained. Accordingly, the exciting force can be calculated based on the actual valve dimensions and the operating condition.

Generally, the amount of abrasion due to the rubbing of valve parts for exciting the valve in its natural frequency can be described as shown in Equation (4). After the valve resonant frequency and the dynamic vibration characteristics such as amplification factors are calculated, the vibratory amplitude can be expected corresponding to the exciting force. This estimation of frequency and damping effect is very important.

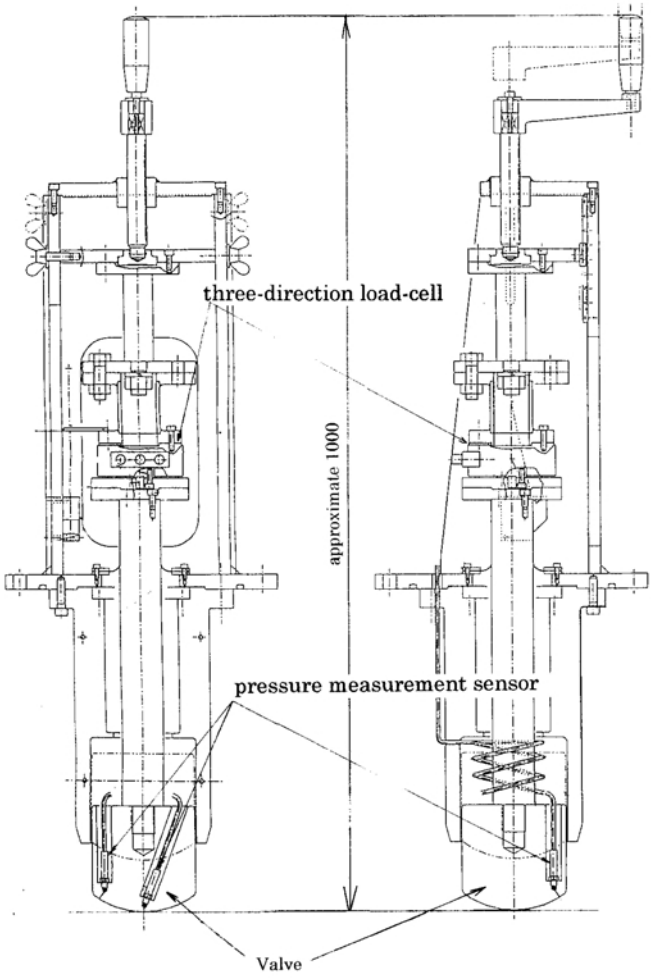

Figure 4. Detail of Test Valve.

$$\delta = K \cdot P \cdot S \cdot \omega \cdot \Delta t \cdot N \cdot T \quad (4)$$

where:
δ = Abrasion quantity
K = Constant number depends on material hardness
P = Intensity at contact area
S = Vibratory amplitude at contact area
ω = Frequency
Δt = Time during contact
N = Contact number
T = Operation time of turbine

In order to estimate the resonance frequency and vibration mode of the valve, vibratory analysis based on the modeling of beam elements shown in Figure 7 was carried out and results of the calculation were compared with the actual frequency measured by the hammering test as shown on Table 1. The test results agree with the calculated ones.

By using the value of Equation (4), the abrasion increase was calculated for long operation in the most severe case where the valve stem always contacts the bushing as shown in Figure 8.

It was concluded that this developed valve can be used for more than 10 years without changing the related parts. This valve has high reliability against abrasion that the allowable clearance can be defined as 1.5 times that of the original clearance between the valve stem and the bushing, even if this severe operating condition continues.

Chattering Phenomenon of Governing Valve

The criteria of valve chattering phenomena (unstable vibration) can be evaluated by Equation (5). Generally when the damping

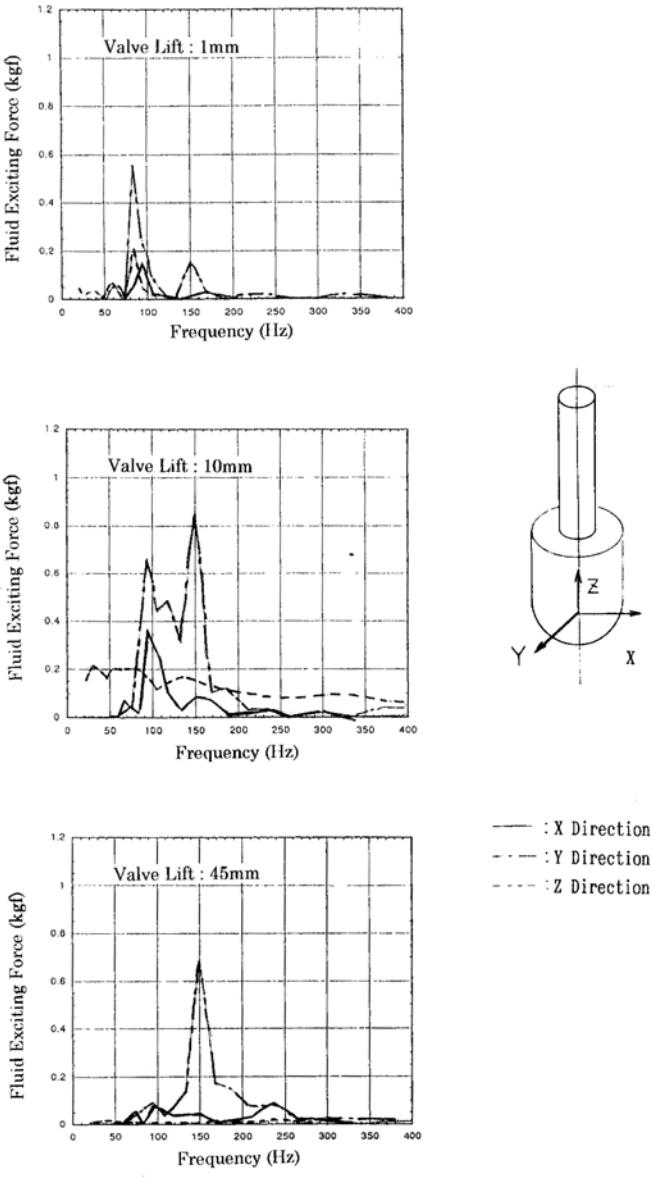

Figure 5. Typical Measurement Data.

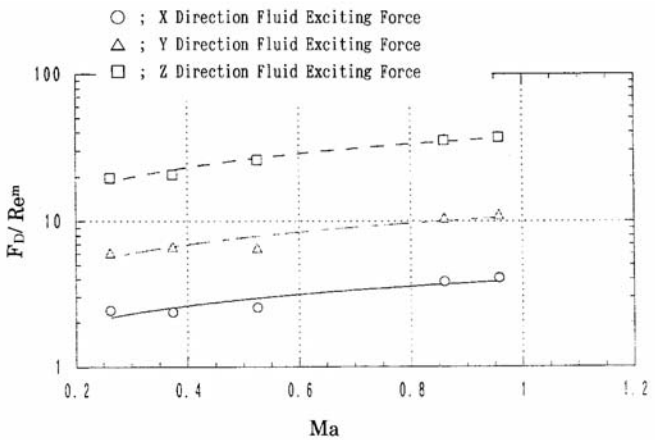

Figure 6. Relation Between Mach Number and Fluid Exciting Force.

coefficient of the governing valve (ζ) is larger than the exciting force of the steam at valve passing (ξ), the vibratory system of the

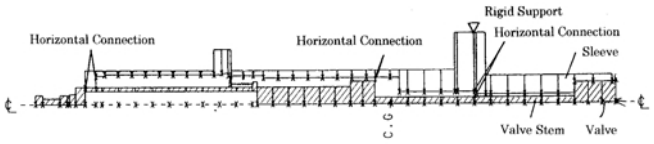

Figure 7. Beam Model for Valve Assembly.

Table 1. Resonant Frequency of Calculation and Hammering Test.

mode	calculation	Hammering Test	
	resonant frequency (Hz)	resonant frequency (Hz)	damping ratio
1	33.2	32.8	0.27
2	59.6	64.6	0.019
3	115.8	107.5	0.002

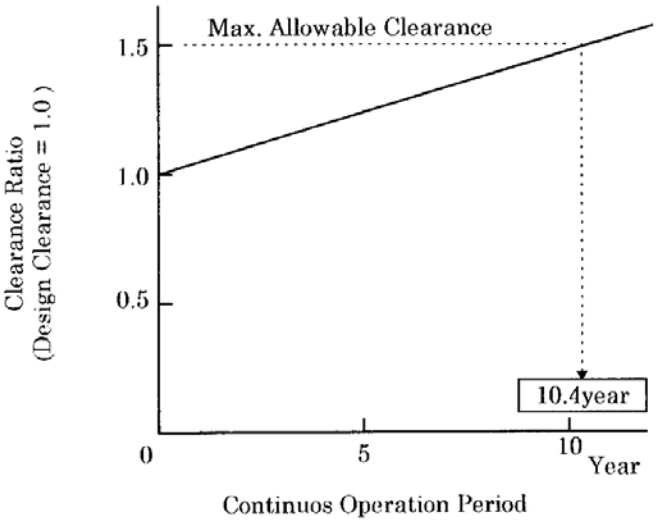

Figure 8. Relation Between Abrasion and Operation.

valve is stable. ζ can be found by the modified equation of Weaver and Ziad (1980) under the following assumption:

- Initial opening ratio of valve X_0 >> vibration amplitude X
- X can be expressed $X \propto e^{i\omega t}$

$$\zeta = \frac{1}{4}\beta\left(\alpha + \frac{\eta\alpha_0}{C_c X_0}\right)\cdot X_0^2 \cdot \frac{C_d}{\eta^3}\cdot C_c^2 \cdot \sqrt{\Delta P}\cdot\sqrt{\frac{\kappa}{(\kappa-1)\psi}} \qquad (5)$$

where:
β = Mass ratio
η = Area of upstream pipe
C_d = Contraction coefficient due to drag with vortex, etc.
ΔP = Pressure ratio
ψ = Nondimensional energy loss by turbulent flow
α_0 = Inertia coefficient
C_c = Flow coefficient
κ = Adiabatic coefficient

ξ can be found by the continuity equation and Bernoulli equation as below:

$$\xi = \frac{\Delta F}{d\dot{x}}\frac{1}{2\omega_o m} = \frac{\rho\cdot u\cdot L\cdot S_v}{Ma^2-1}\frac{1}{X_0}\frac{1}{2\sqrt{K\cdot m}} \qquad (6)$$

where:
ΔF = Variable force
ω_0 = Natural frequency of valve
S_v = Sectional area of valve
$d\dot{x}$ = Differential displacement
m = Valve mass
K = Support stiffness of valve

According to Equations (5) and (6), if the relation between ΔP and X_0 are found, the stability limitation for chattering vibration can be evaluated.

In order to find this relation, a model test was carried out by using the test device shown in Figure 9. The displacement of the valve was measured by a laser displacement meter. The valve vibration of axis direction was measured by an acceleration meter. The resonant frequency, the pressure ratio, and the opening ratio of the valve were applied as test parameters. Measurement data at the occurring unstable vibrations are shown in Figure 10. According to this figure, it was found that the phase difference between the pressure and the vibration around the valve is about 90 degrees. This phenomenon means the pressure around the valve body will be the self-exciting force for the governing valve vibration. Based on the measurement data, the criteria map for chattering vibration of the test model was found as shown in Figure 11.

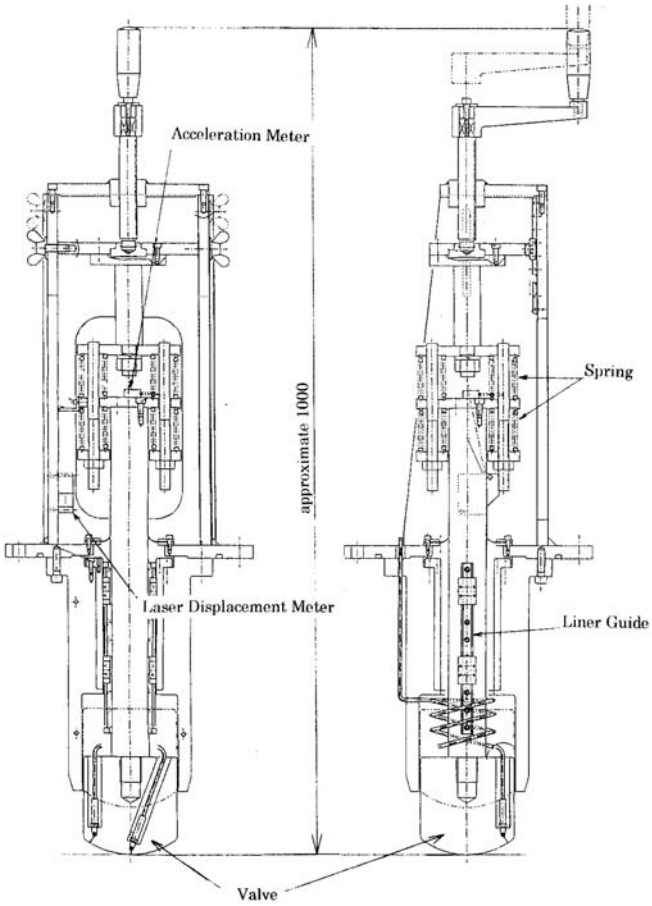

Figure 9. Detail of Test Valve.

The maximum exciting force for the actual valve of the steam turbine was found by using the test data and it was calculated below $\zeta = 0.04$. This value is small enough against the damping ratio of the actual valve. From this result, it is concluded that chattering vibration of the actual turbine never occurs.

Through the above evaluations concerning abrasion and the chattering phenomenon for the governing valve, it can be explained that the governing valve of the developed steam turbine is reliable enough for capacity increases.

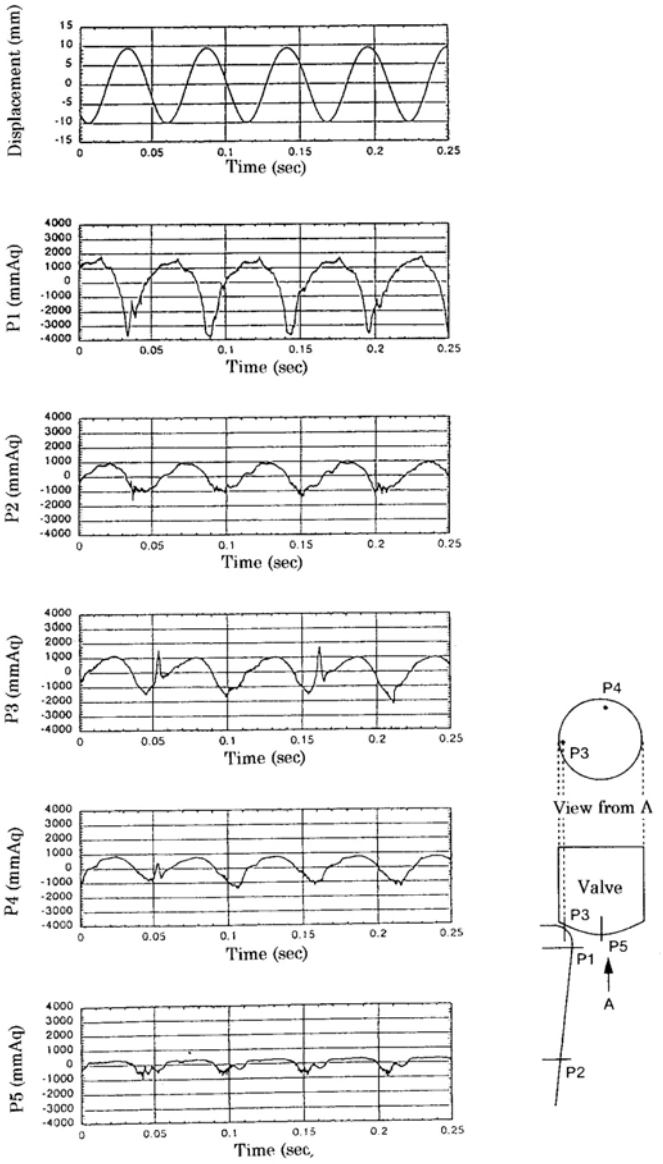

Figure 10. Measurement Data at Occurring Unstable Vibration.

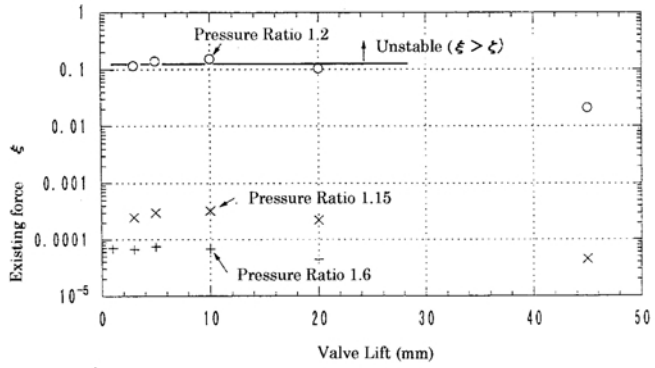

Figure 11. Evaluation Map for Chattering.

RELIABILITY IMPROVEMENT FOR BLADE

One of the most serious damages to the blades during long-term operation is the erosion on the profile surface. Especially when exhaust vacuum pressure is low in order to achieve high performance, protection against erosion for the low-pressure stage blades is important.

In order to prevent drainage erosion damage, the use of silver brazing of the stellite plate is applied to the last stage blades as one of the solutions. However, it was found that the silver brazing causes a decrease in the endurance limit of blade material.

Instead of the stellite plate silver brazing, the following two new technologies, Cr-TiN ion coating and plasma transfer arc (PTA) welding, were developed for the low-pressure stage blades to prevent drain attack erosion.

Cr-TiN Ion Coating

Cr-TiN ion coating has been applied to the low-pressure stage of steam turbine blades since 1987 in one ethylene plant. After eight years' operation, it was confirmed that the blades' profile surface had no erosion. Figure 12 shows the typical microstructure of the coated section applied for this plant. Recently, in order to improve the anti-erosion characteristic further, the modified Cr-TiN ion coating with an increased coating thickness of TiN was applied for other steam turbines.

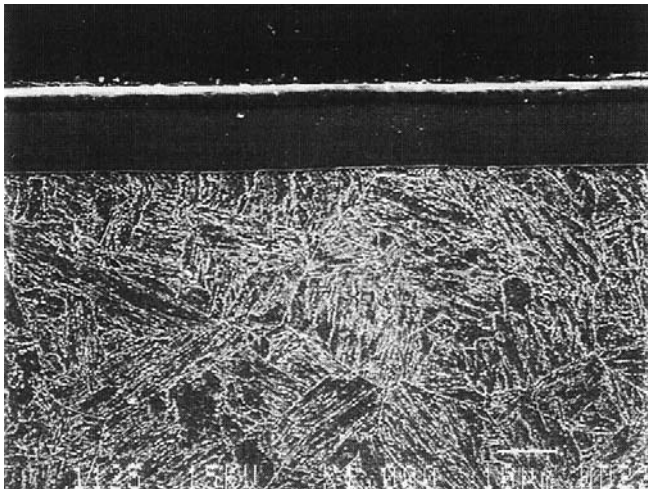

Figure 12. Microstructure of Cr-TiN Coated Steel.

However, increasing the coating thickness of Cr-TiN excessively causes the occurrence of a crack due to the inner stress in the TiN layer. Therefore, in order to improve the anti-erosion characteristic without decreasing the endurance limit even in a heavy-erosion environment, the plasma transfer arc welding method has been developed.

Stellite Welding by Plasma Transfer Arc Method

According to the plasma transfer arc (PTA) technology, a very thin metal welded layer can be formed on the surface of the base material by pouring stellite powder inside the plasma arc between the base material and the torch. The PTA device schematic is shown in Figure 13. In order to evaluate the possibility of PTA application to the actual turbine blade, the welding condition, the erosion characteristic, and the endurance limit were confirmed by examination of a test piece.

Figure 14 shows the relation between the surface hardness of the welding bead and the rate of dilution for the test parameters such as welding location and width of bead oscillation. According to these figures, it was found that the test piece with smaller welding oscillation width has the higher hardness and the hardness changes as the welded bead becomes smaller. From these examinations, the welding conditions were determined. Below 10 percent rate of dilution and narrow oscillated bead, the hardness of the welded area is above 400 Hv of the stellite plate by silver brazing.

Figure 15 shows the result of the erosion acceleration, based on ASTM G32-77 (1998), on the test device shown in Figure 16. It was found that the decrement of weight due to erosion after 10

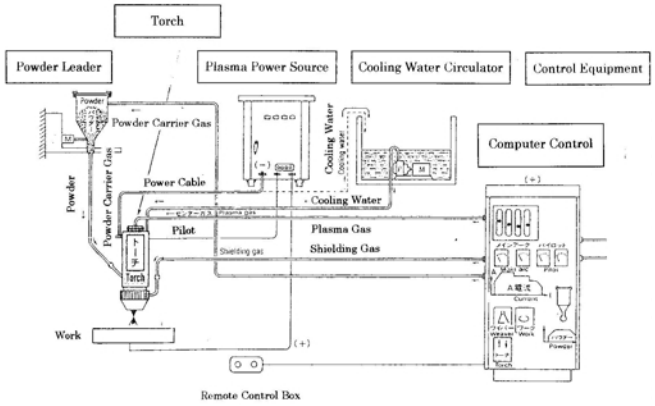

Figure 13. Device for PTA.

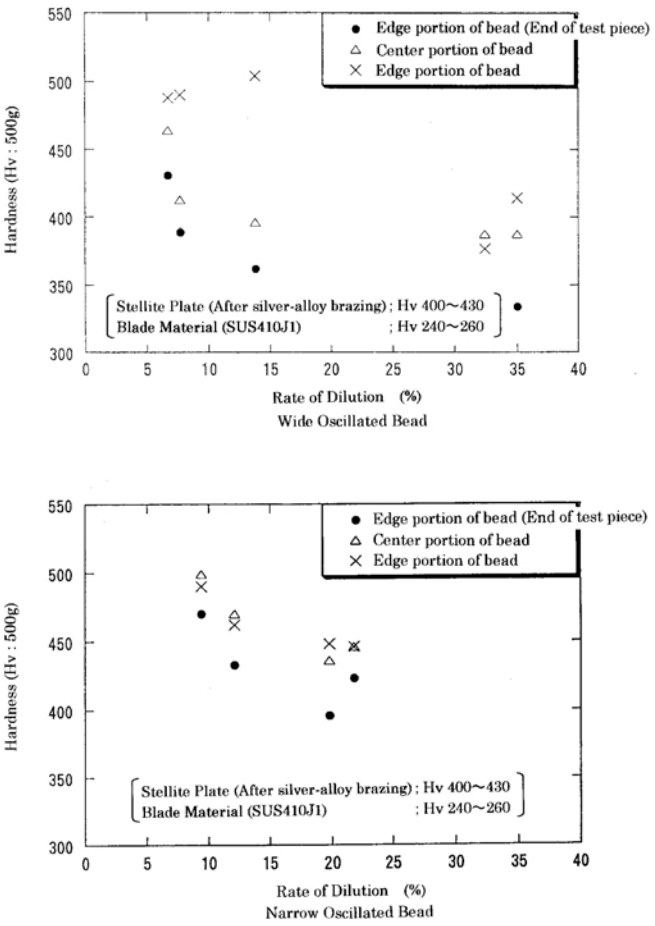

Figure 14. Relation Between Oscillated Bead and Hardness.

hours is about 0.08 ~ 0.29 mg and this value is better than the value of the stellite plate by silver brazing.

Figure 17 shows the examination result of endurance limits. According to this figure, it was confirmed that the endurance limit of the stellite welded base material by PTA is superior to one of stellite plate by silver brazing.

The main cause of decreasing the endurance limit for stellite plate by silver brazing seems to be the crack propagation due to stress concentration around the blowholes in the silver brazing. On the contrary, the defect in the stellite welded layer by PTA was not observed. A preliminary test of PTA technology before applying it to the actual blades was successfully completed and at present this technology is trying to be applied to the actual blades.

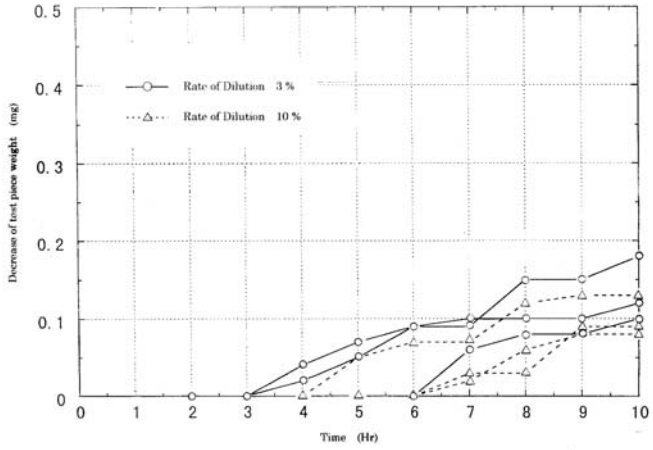

Figure 15. Result of Erosion Examination.

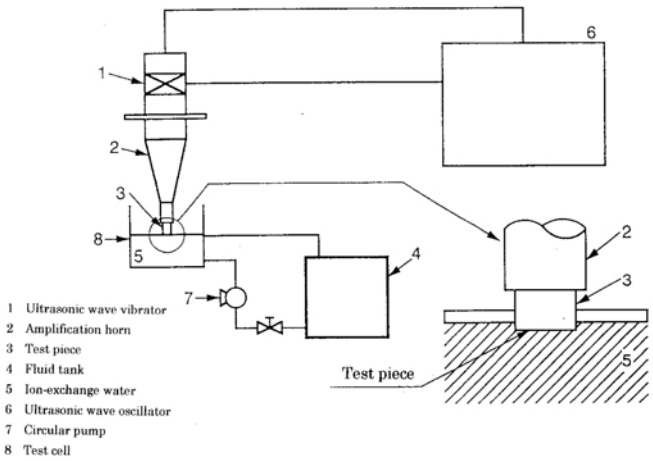

Figure 16. Test Device.

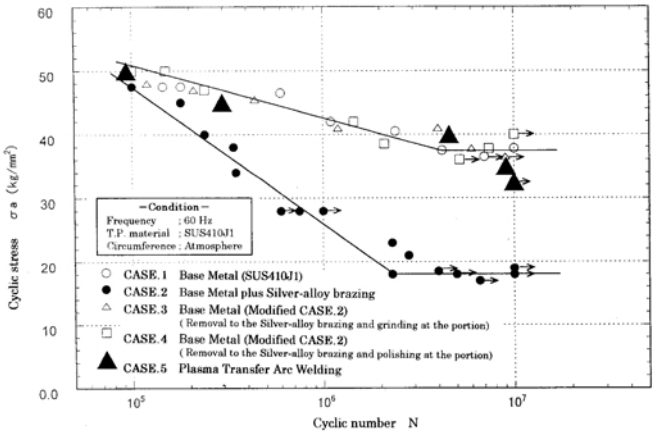

Figure 17. Examination Result of Endurance Limit.

IMPROVEMENT OF PERFORMANCE AND STAGE EFFICIENCY

Generally, the improvement of stage efficiency is most important in order to get high performance from a steam turbine. Figure 18 shows a cross section drawing of the blade path around the high-pressure stages of an extraction steam turbine used in an ethylene plant. Figure 19 shows the result of loss analysis for nozzles and blades in the high-pressure stage. The power loss of the first stage occupies about 60 percent of the total power loss of

the high-pressure stage and the improvement of the first stage performance was carried out to minimize the loss of secondary flow around the first stage nozzles.

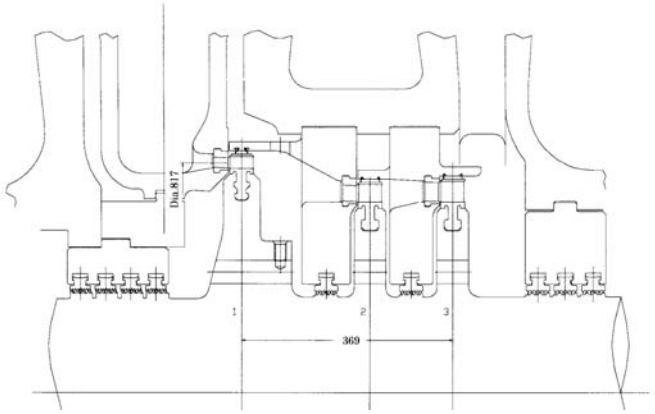

Figure 18. Cross Sectional Drawing of High-Pressure Stage.

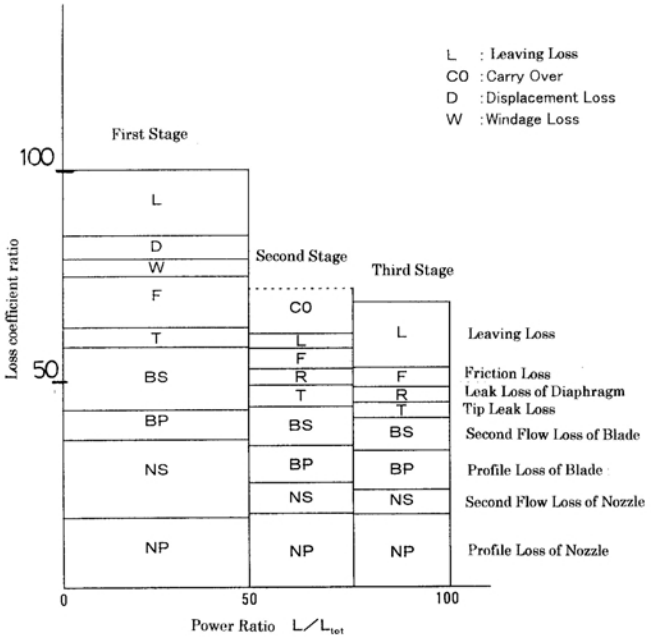

Figure 19. Loss Analysis for Nozzle and Blade in High-Pressure Stage.

In order to reduce the loss of secondary flow for the nozzles, the bow nozzle (a three-dimensional new profile nozzle), shown in Figure 20, was considered. These nozzles are usually manufactured by fine casting. However, in considering the actual application, adjusting the nozzle area suitable for the blade height without changing the profile of the nozzle from the standpoint of cost and delivery was considered. Consequently, the wide orientation of the nozzles to change the throat width was applied. The orientation of the nozzle outlet angle was defined as the basic angle ±3 degrees and the height of the nozzles were classified as two types.

Three-dimensional fluid analysis was performed to evaluate the performance of these nozzles. Figure 21 shows the basic profile figure and Figure 22 shows the velocity distribution on the profile surface. The maximum Mach number of each orientation angle was minimized below 1.2 to reduce loss. The analysis confirmed that this wide orientation never affected the nozzle performance.

Figure 23 shows a three-dimensional figure and the distribution of profile load ratios for the bow nozzle. The profile figure was

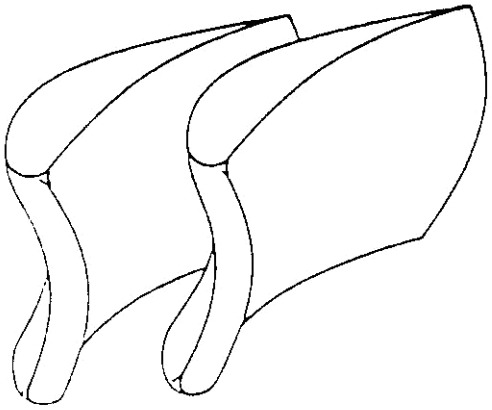

Figure 20. Figure of Bow Nozzle. (View from steam inlet side.)

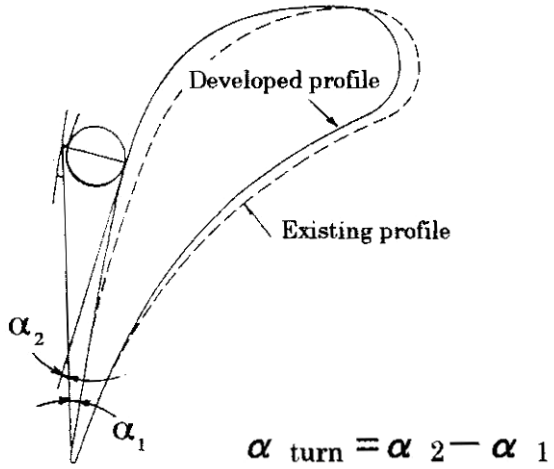

Figure 21. Basic Profile Figure.

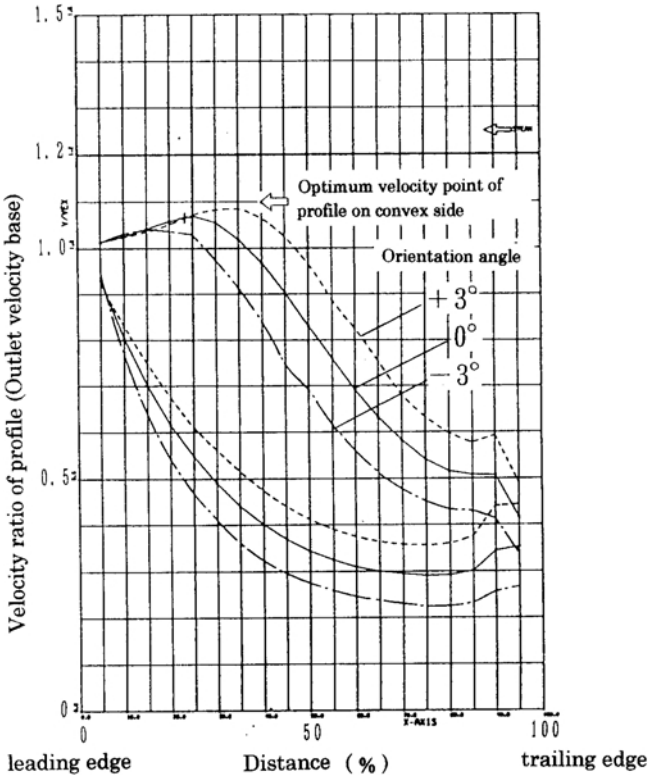

Figure 22. Velocity Distribution on Profile Surface.

modified so that the profile load in the mean height does not increase in comparison with a two-dimensional parallel nozzle to minimize the profile loss.

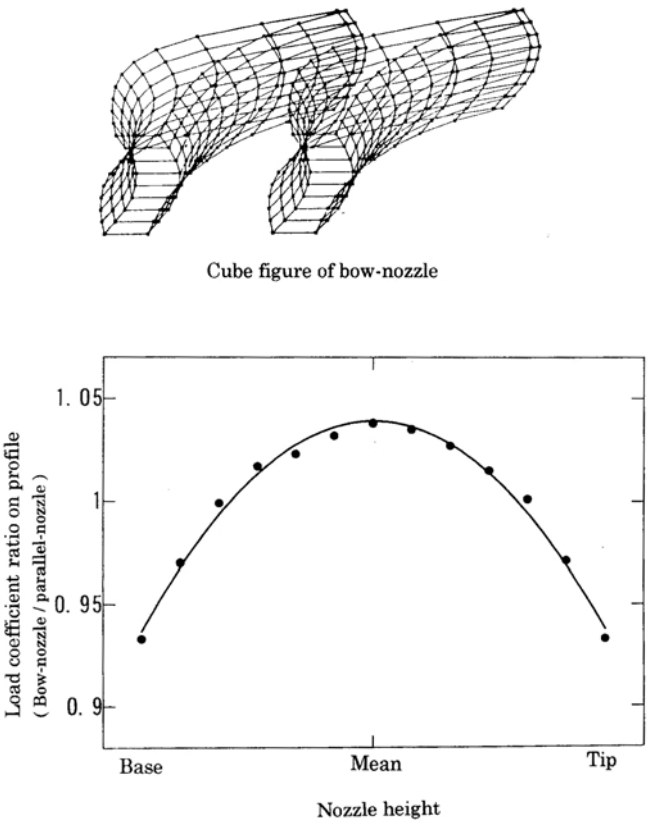

Figure 23. Distribution of Profile Load Ratio.

Figure 24 shows the distribution of static pressure for the developed bow nozzle in comparing the conventional parallel nozzle. No flow stain and no separation were confirmed.

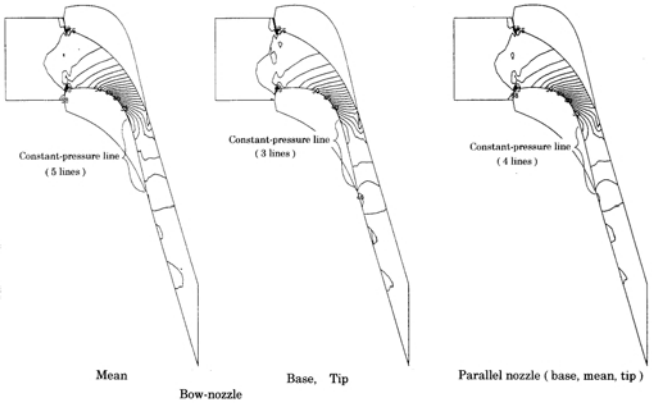

Figure 24. Distribution of Static Pressure in Steam Passing Area.

A cascade test was carried out to measure the performance of the combination of the developed bow nozzle and the related blades. Figure 25 shows the test result of loss distributions in comparison with conventional parallel nozzles. From this figure, it was confirmed that the loss of the bow nozzle was almost at the same level along the nozzle height and the loss of the vortex core due to the second flow was obviously decreased.

Figure 26 shows the influence of orientation angles on the performance. The minus angle orientation seemed to decrease the loss

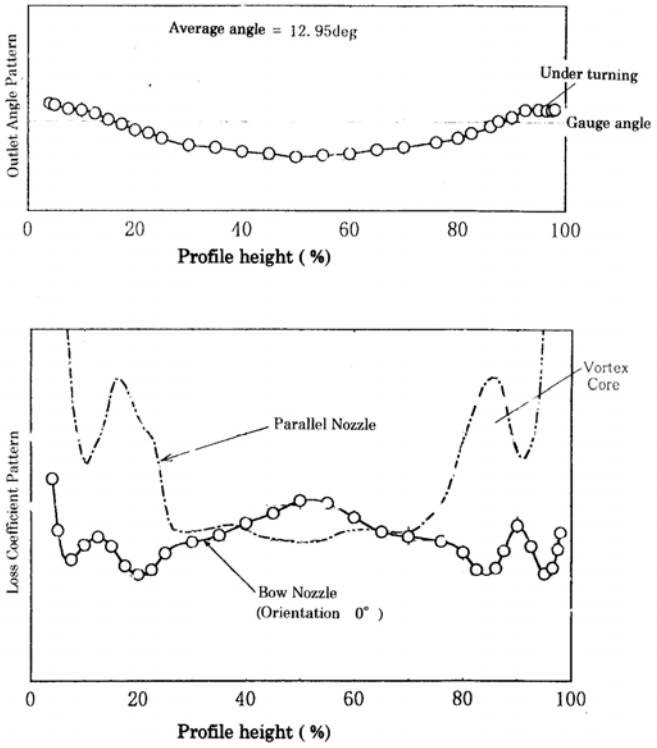

Figure 25. Loss Distribution (Bow Nozzle and Parallel Nozzle).

because the interference with the second flow in the middle of height was controlled according to the flow acceleration. As a result of this test, it was confirmed that the effect on performance due to the change of nozzle orientation was small. The expected increase of stage efficiency by using the bow nozzle is more than 2 percent.

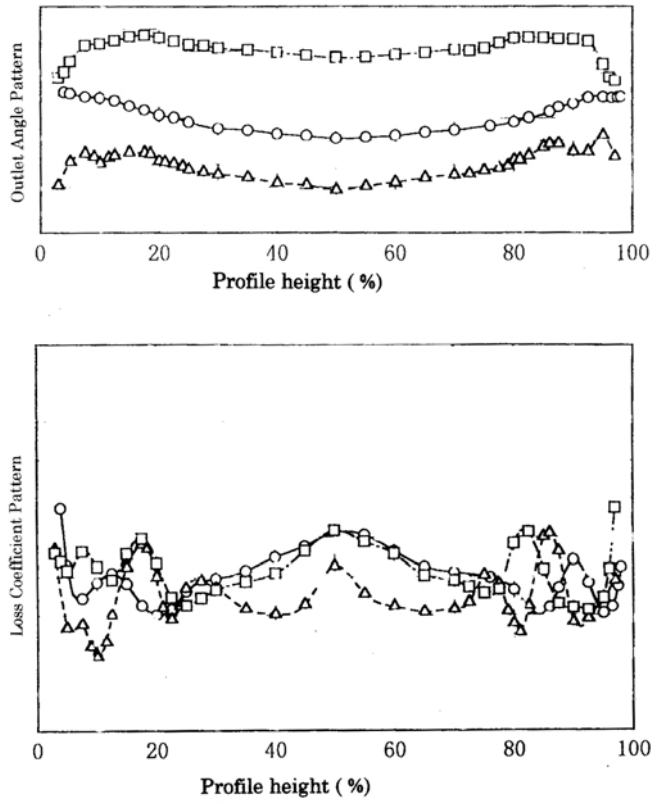

Figure 26. Influence of Orientation Angle.

The improvement of the blades' efficiency in using the developed bow nozzle was also considered. In using the parallel nozzle, the overturning occurs at both ends of the nozzle, as shown in Figure 27. However, in using the bow nozzle, the underturning has the effect of decreasing the loss of secondary flow and the estimated increase of blade efficiency is about 0.5 percent. The increase of efficiency of the stage is summarized in Table 2.

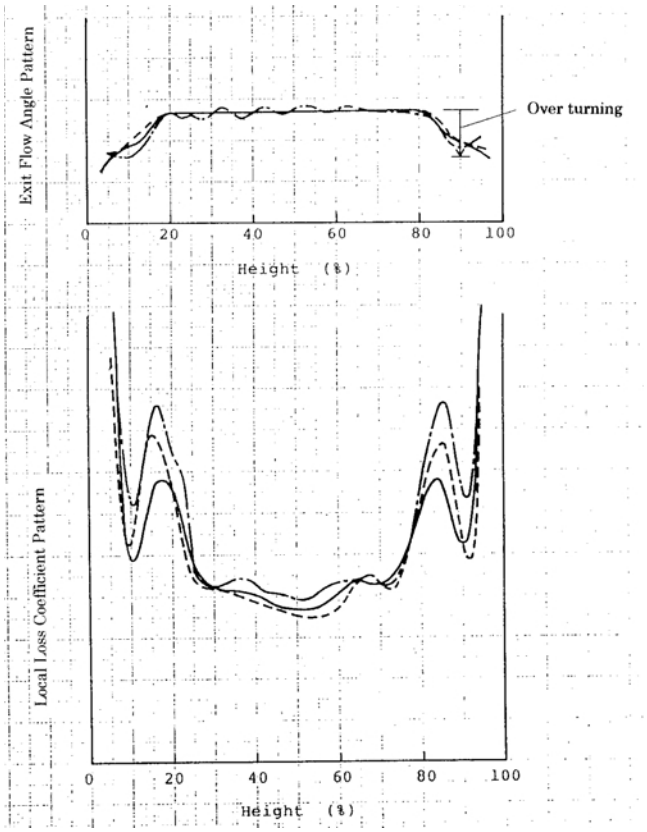

Figure 27. Loss Distribution of Parallel Nozzle.

Table 2. Performance Improvement by the Bow Nozzle.

	Improvement of each nozzle and blade	Load Distribution	Stage Improvement
Nozzle	2.2%	0.7	1.5%
Blade	0.5%	0.3	0.2%
Total			1.7%

PERFORMANCE IMPROVEMENT OF LABYRINTH SEALS

Many studies have been performed on labyrinth seals used for rotating machines. The new technology labyrinth seal was designed by application of a slanting labyrinth fin angle.

In order to obtain the leakage performance of a slanting labyrinth seal, an air test was carried out by using the model shown in Figure 28. In this test, the groove depth, fin number, and seal clearance were changed as the parameter under the condition that the tip thickness and slanting angle were fixed. Figure 29 shows the relation between the flow coefficient and the clearance in comparison with the characteristics of the original labyrinth.

Slanting labyrinth seals (Type I, II, and III) have superior seal performance to the original one, below clearance ratio of 1.6, and Type III has the best seal performance. In the range of clearance ratios larger than 1.6, the seal performance of Type I and II become inferior to the original one. The reason for the leakage characteristics difference is that the kinetic energy of jet flow from

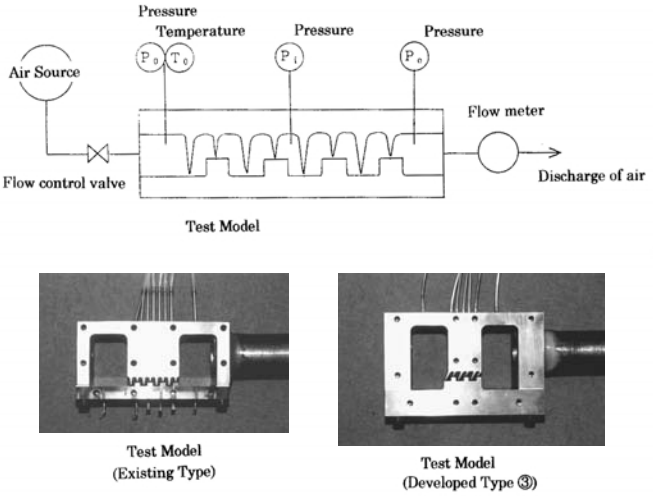

Figure 28. Test Model of Labyrinth Seal.

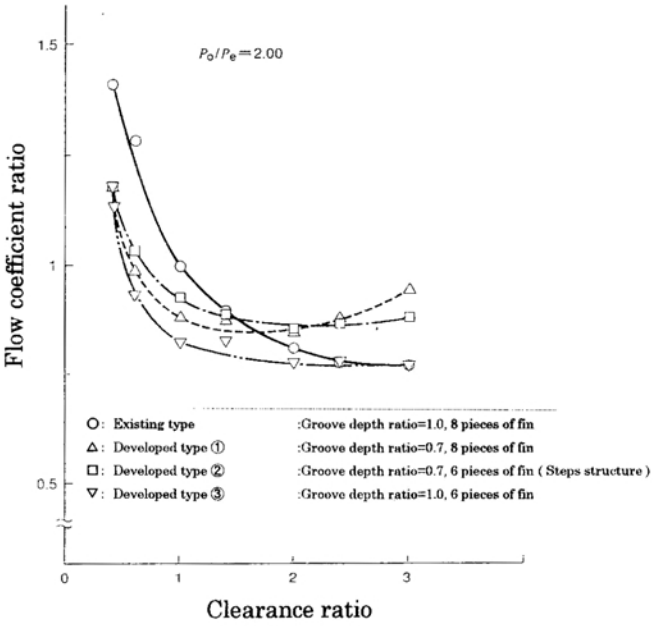

Figure 29. Discharge Coefficient of Slanting.

the long fin is carried over and then utilized for inlet energy of the short fin.

Figure 30 shows the flow visualization result of the labyrinth seal for a clearance ratio of 1.0. In comparison with the original labyrinth seal, a larger flow contraction was observed at the tip of the slanting labyrinth seal, therefore, the leakage coefficient decreased.

The tangential component of axial steam flow at the labyrinth seal sometimes works as self-exciting force on the rotor. In the event that the cross term spring coefficient is larger than the damping coefficient, there is the possibility of unstable vibration occurring. Table 3 shows the calculation result of exciting force for a labyrinth seal based on the actual steam condition. From this table, it is confirmed that the slanting labyrinth seal has more stable characteristics than the original one. This slanting labyrinth seal has been applied for a lot of actual steam turbines.

CONCLUSION

In order to respond to the recent requirements for capacity increase and the continuous long-term operation in ethylene plants, the improvement of the reliability and performance of steam turbines was introduced.

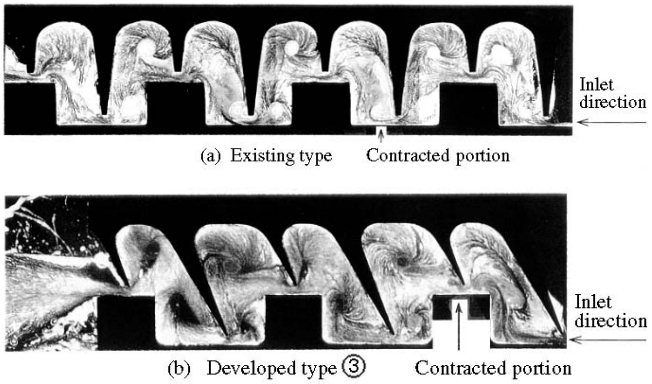

Figure 30. Visualization of Flow Line.

Table 3. Calculation Results of Exciting Force for Labyrinth Seal.

Seal type	Existing type	Developed type ①	Developed type ②	Developed type ③
Flow coefficient ratio	1.0*	0.76	0.81	0.73
Ratio of inlet press. to outlet press.	3.7	3.7	3.7	3.7
Temp.(°C)	480	480	480	480
Spring constant of stability force (relative ratio of Kxx)	1.0	0.96	1.05	0.74
Spring constant of exciting force (relative ratio of Kxy)	1.0	0.91	1.17	0.83
Damping constant of damping force (relative ratio of Cxx)	1.0	1.09	1.29	0.81
Unstable force on seal portion (relative ratio of Kxy−Cxx ω)	1.0	0.89	1.16	0.83
Calculation condition	Rotor speed Ω : 6100rpm Natural frequency of rotor ω :4200rpm Swirl ratio Ω/ω : 0.6			

*: Flow coefficient ratio is 1.0 under condition that clearance ratio is 0.6.

A newly designed governing valve has good characteristics against abrasion and unstable vibration such as chattering. A new method of stellite welding for low-pressure stage blades has been developed successfully for an actual application.

A bow nozzle for the high-pressure stage can improve efficiency by wide range nozzle orientation. The better sealing effect of slanting seals was also confirmed.

REFERENCES

ASTM G32-77, Updated G32-98, 1998, “Standard Test Method for Cavitation Erosion Using Vibratory Apparatus,” American Society for Testing and Materials, West Conshohocken, Pennsylvania.

Weaver, D. S. and Ziada, S., 1980, “A Theoretical Model for Self-Excited Vibrations in Hydraulic Gates, Valves, and Seals,” Transactions of the ASME, *102*, pp. 146-151.

BIBLIOGRAPHY

Takenaga, H., Sasaki, T., Hata, S., and Isumi, O., 1998, “Performance Improvement of Seals for Mechanical Steam Turbines,” Mitsubishi Heavy Industries, Ltd., Technical Review, *35*, (3).